Assimilation of AIRS and IASI at ECMWF

Andrew Collard

ECMWF, Shinfield Park, Reading
RG2 9AX, United Kingdom
andrew.collard@ecmwf.int

ABSTRACT

The kilochannel infrared sounders, AIRS and IASI, are important contributors to the ECMWF data assimilation system. This class of instrument can provide information with high accuracy and vertical resolution through the use of their large number of low-noise channels with overlapping Jacobians. The current use of these instruments requires sub-sampling spatially (e.g., cloud detection, thinning) and spectrally (channel selection). The choices made in this regard are examined and the potential for future increased use of the data are explored.

1 Introduction

On 4th May 2002 the AIRS (Atmospheric InfraRed Sounder, Aumann *et al.*, 2003) instrument was launched on the NASA EOS-Aqua satellite. Operational assimilation of AIRS radiances began at ECMWF in October 2003, this being the first assimilation of data from a kilochannel infrared sounder into an operational numerical weather prediction (NWP) system.

A second such instrument, IASI (Infrared Atmospheric Sounding Interferometer; Chalon *et al.*, 2001) on the EUMETSAT MetOp-A platform, was launched on 19th October 2006 and data from this was first assimilated operationally at ECMWF on 12th June 2007. Further launches of IASI instruments on MetOp satellites and of CrIS (Bloom, 2001) on NPOESS satellites will continue the availability of such data for the foreseeable future. With the exception of AIRS — a grating spectrometer — all of these instruments are Fourier transform spectrometers (FTS). The properties of these three sounders are summarised in Table 1

It is worth noting that kilochannel infrared sounders have flown prior to the launch of AIRS, the first being IRIS (Infrared Radiometer Spectrometer Interferometer and Spectrometer) on NIMBUS 3 & 4 in 1969–70 (Hanel *et al.*,1971). More recently IMG (Interferometric Monitor for Greenhouse gases; Kobayashi *et al.*, 1999), was flown on the Japanese ADEOS satellite between October 1996 and June 1997. A comparison of data from IRIS and IMG has been used to infer climate signals by Harries *et al.* (2001). Similar instruments have contributed to our understanding of other planets in the solar system, particularly the IRIS instruments on the Voyager probes that visited the giant planets in the 1980s (Hanel *et al.*, 1977). In addition many investigations from aircraft and ground-based platforms preceeded the launch of AIRS, in particular the HIS (High Resolution Interferometer Sounder) instrument developed by the University of Wisconsin (e.g., Smith *et al.*, 1995).

The advantage of the kilochannel sounders over the preceeding HIRS system is illustrated in Fig. 1. Here part of a simulated IASI spectrum with a line-resolving resolution of 0.5cm^{-1} is compared with the filter response functions of the HIRS instrument on NOAA 15. It is apparent that the HIRS filter widths are such that fine spectral structure is lost and also that the number of channels measuring the atmosphere is two orders of magnitude higher for IASI. Fig. 2 shows the AIRS temperature Jacobians[1] for the same region of the spectrum

[1]The Jacobian matrix $\mathbf{H}$ is the derivative of the vector of observed radiances $\mathbf{y}$ with the state vector $\mathbf{x}$, such that $\mathbf{H} = \nabla_x \mathbf{y}(\mathbf{x})$.

Parameter	Advanced Sounder		
	AIRS	IASI	CrIS
Instrument type	Grating Spectrometer	Interferometer	Interferometer
Platform	Aqua	MetOp-A/B/C	NPP & NPOESS
Satellite Agency	NASA/JPL	EUMETSAT/ CNES	NOAA IPO
Spectral range (cm^{-1})	649–1135; 1217–1613; 2169–2674	Contiguous 645–2940	650–1095; 1210–1750; 2155–2550
Number of channels	2378	8461	∼1300
Unapodised spectral resolving power	1000–1400	2000–4000	900–1800
Spectral sampling	$\sim \nu/2400$	0.25 cm^{-1}	0.625/1.25/2.5cm^{-1}
Spatial footprint (km)	13.5	12	14
(Nominal) Launch date	4th May 2002	19th Oct 2006	2009 & 2012

Table 1: Summary of the instrument characteristics of current and future kilochannel infrared sounders (updated from Saunders, 2001).

from which it can be seen that the IASI Jacobians are slightly narrower than the HIRS equivalents, but that the real power of instruments such as AIRS and IASI is the large number of overlapping Jacobians. It is primarily the assimilation system using the information from the differences in these Jacobians that allows greater vertical resolution to be extracted from kilochannel sounder measurements.

Linear simulations of IASI retrieval performance (Collard, 2001; Collard and Healy, 2003) illustrate the much improved retrieval accuracy and resolving power that one would expect from these instruments. Fig. 3 compares expected retrieval accuracy (using an NWP 6-hour forecast as *a priori* data) for IASI and HIRS. The retrieval accuracy for IASI is far superior to that for HIRS, a large part being due to the improved vertical resolution of the former.

To illustrate the comparative vertical resolutions of the two instruments, Fig. 4 shows a temperature perturbation that was used in an study by Prunet *et al.* (1998). This profile was one of those that Prunet *et al.* extracted from a study by Rabier *et al.* (1996) which identified error structures in the initial atmospheric state of an NWP model run that would grow rapidly with time and would result in erroneous forecasts. These error structures were important in the failed forecasting of the re-intensification of the remnants of Hurricane Floyd over Brittany and SW England in September 1993. It can be seen that IASI performs much better than HIRS at retrieving fine structure in the temperature profile. Particularly the 3km wide temperature spike at 4km altitude is much better represented for the former instrument. It should be noted, however, that studies by McNally (2002) indicate that these “sensitive regions” are often cloud contaminated, especially with low cloud.

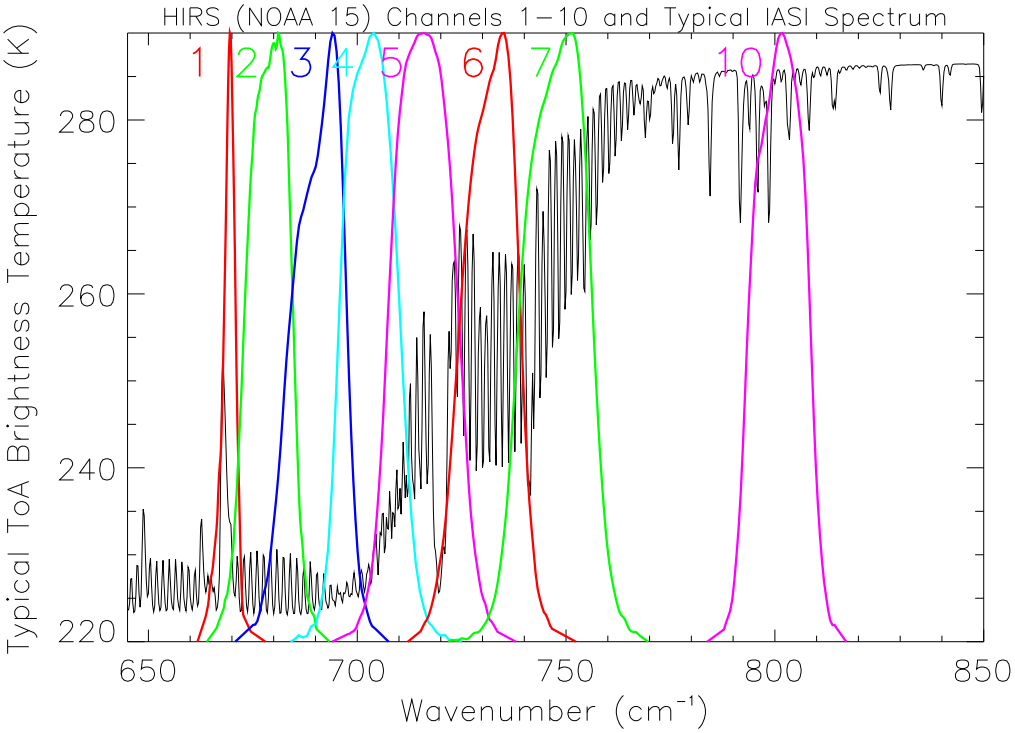

Figure 1: A comparison of a portion of a typical simulated IASI spectrum with the instrument spectral response functions (ISRF) for HIRS in this region. The smoothing out of spectral features by the HIRS ISRF is clear.

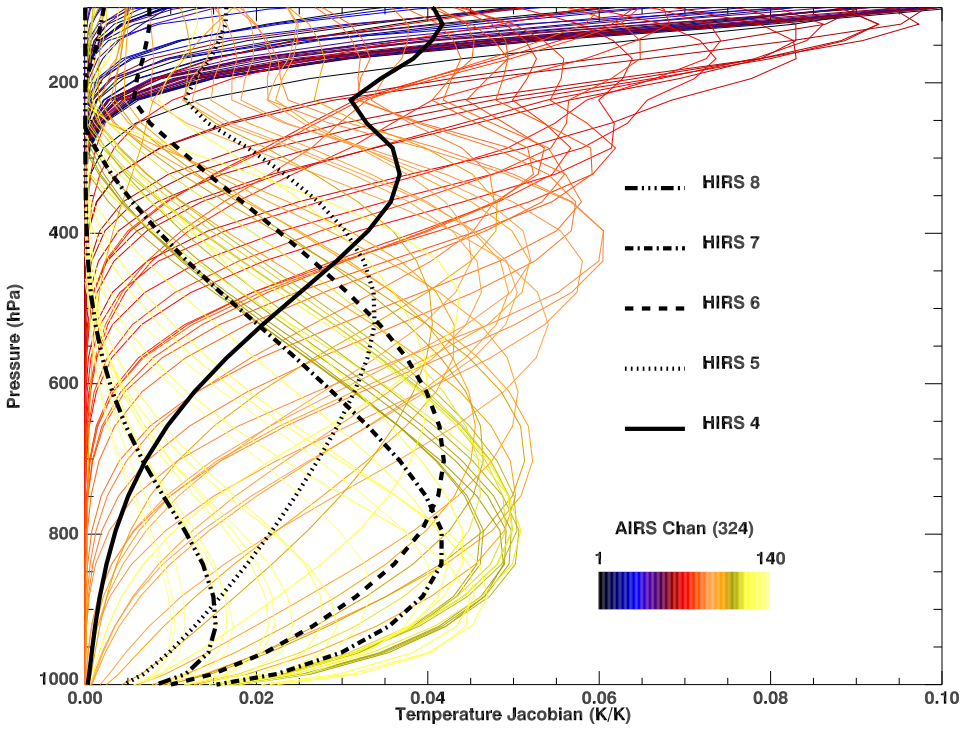

Figure 2: Typical AIRS Jacobians in the 15μm CO_2 band from the subset of 324 channels that are distributed in near-real-time compared to HIRS Jacobians. The AIRS Jacobians are only slightly sharper than the equivalent HIRS ones but the number of overlapping Jacobians may be used to obtain high vertical resolution from AIRS observations.

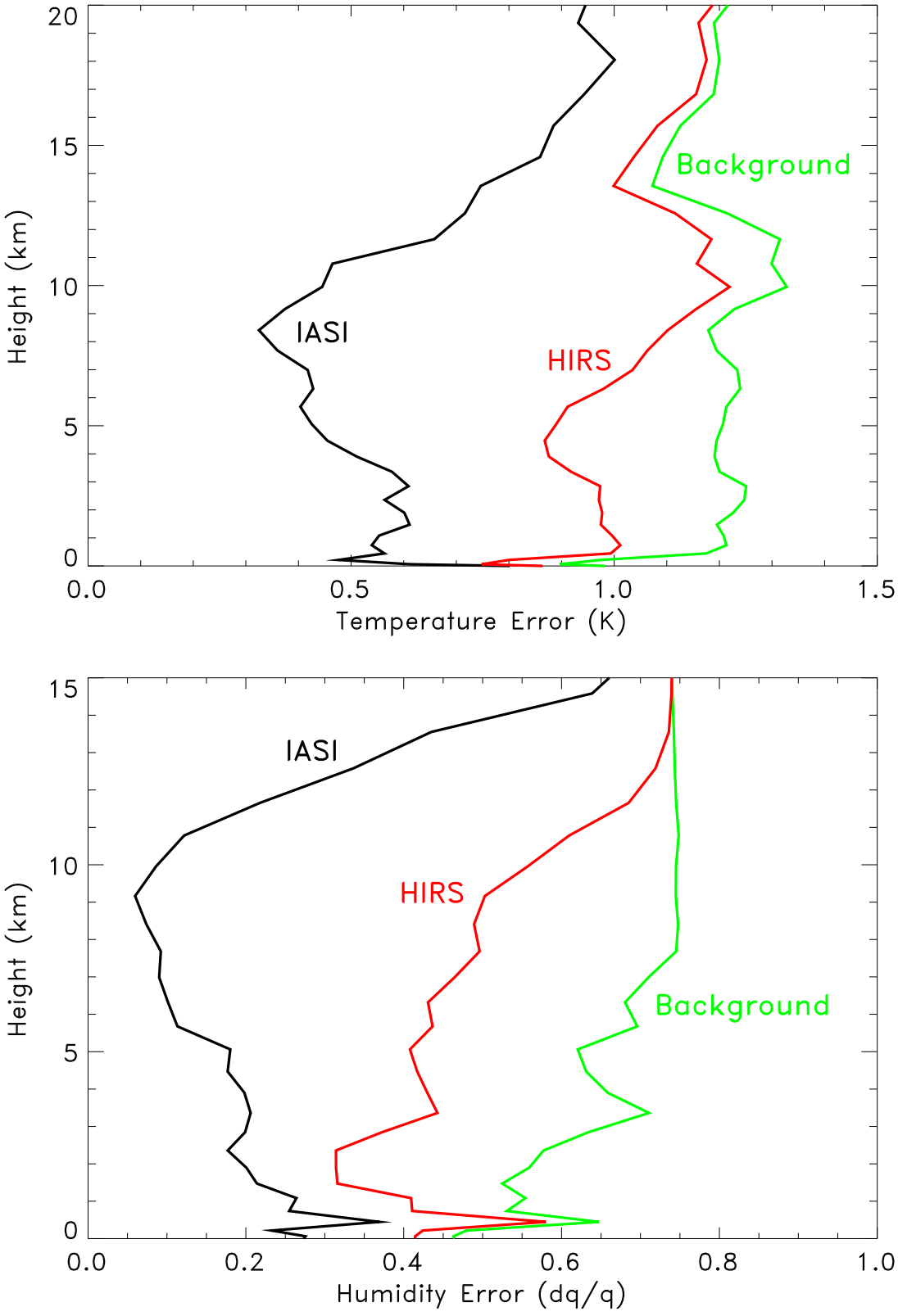

Figure 3: Simulated IASI and HIRS temperature and humidity retrieval accuracies.

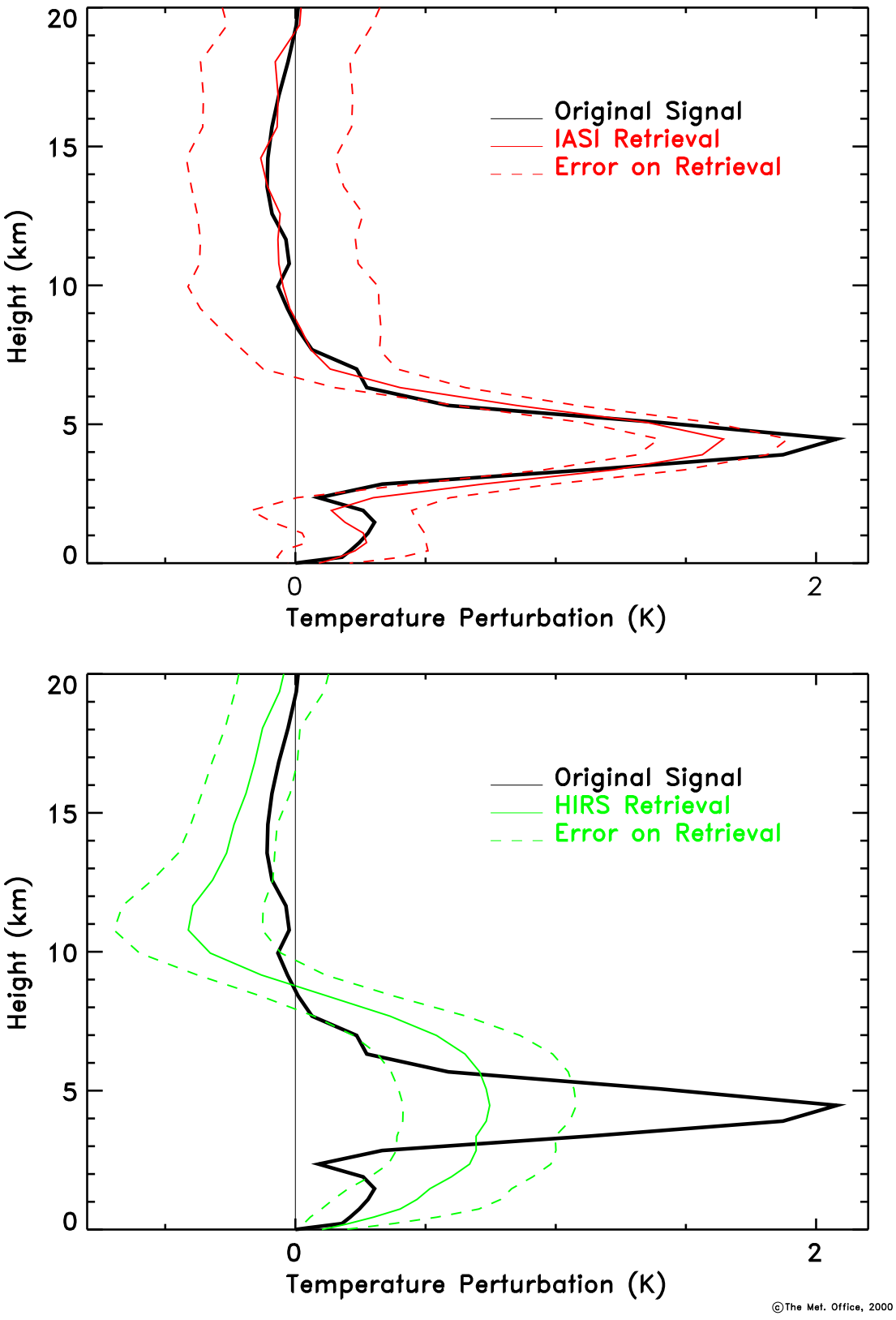

Figure 4: One of the "Rabier curves" used by Prunet et al. (1998) and the corresponding expected profiles that would be retrieved by the HIRS and IASI instruments. The error bars are the respective instrument plus forward model noise projected into retrieval space.

	AIRS	IASI
No. Channels Received	324	8461
No. Channels Monitored	324	366
Max. No. of Channels Actively Assimilated	155	166
Spatial Restrictions	Sea Only for $\lambda < 14.14\mu$m	Sea Only
Spectral Bands	15μm CO_2 band, longwave window, H_2O band, 4.5μm CO_2 band ($\lambda > 4.45\mu$m)	15μm CO_2 band
Spatial Sampling (before thinning to ~120km)	Warmest FOV (in longwave window) per AMSU FOV	Detector 1

Table 2: A comparison of the operational configurations for the assimilation of AIRS and IASI data at ECMWF as of September 2007.

2 Current Operational Configuration of AIRS and IASI at ECMWF

AIRS and IASI are assimilated operationally at ECMWF in a similar but not identical manner. The main differences between the implementations are shown in Table 2. The initial implementation of AIRS is described by McNally *et al.* (2006).

The assumed errors for AIRS and IASI are the same (i.e., channels with the same wavelength have the same assumed error). These are shown in Fig. 5 in comparison with the measured AIRS instrument noise and the standard deviation of the observed−calculated differences ("first-guess departures") at ECMWF. The errors are 0.4K in the important regions sensitive to upper-tropospheric and lower-stratospheric temperature in the 15μm CO_2 band, while they need to be inflated to 2K in the H_2O band. This will be discussed in more detail below.

2.1 Channel Selection

Processing the complete AIRS or IASI spectrum is inefficient and would impose an infeasible burden on the assimilation system. Sophisticated methods for compressing the available information have been suggested and are reviewed in Section 3.3, but in current operation systems a simple channel selection is employed. For each instrument two channel selections are used: a selection of channels which are routinely monitored and a subset of these channels which are actively assimilated. The monitoring channels which are not assimilated allow bands that are not actively assimilated to be inspected thus giving additional insight of instrument and model performance plus they form a pool of potential channels for active assimilation at a later date.

The AIRS monitored channels comprise a set of 324 channels chosen and distributed by NOAA/NESDIS (Susskind *et al.*, 2003; Goldberg *et al.*, 2003). These channels were chosen based on the width of each channel's Jacobians, the instrument noise for each channel, the amount of interference from unwanted species, and the effect each channel has on retrievals. 324 channels were chosen such that the retrieved spectrum reproduced the observed spectrum with an accuracy equal to the instrument noise.

Of the 324 monitored AIRS channels, up to 155 may be assimilated (depending on the inferred cloud top height). Three regions of the spectrum are not considered for active assimilation:

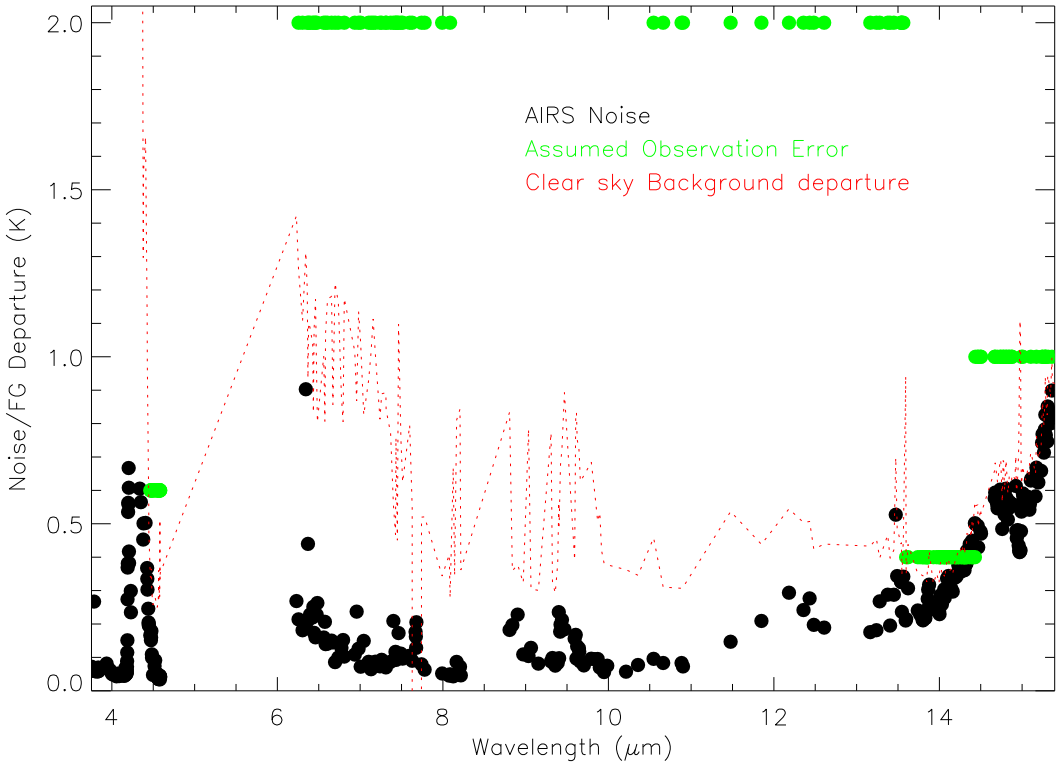

Figure 5: A comparison of the AIRS instrument noise and the assumed observational noise in the assimilation of AIRS radiances.

- Wavelengths less than 4.45μm which may be affected by solar radiation and non-LTE effects in the daytime (but which are not currently used at night either).
- The ozone band around 9.5μm.
- Channels with large upper stratospheric contributions (not used for model specific reasons)

In addition a few channels are removed that have significant effects from CO or N_2O and two channels (300 & 453) which have become very noisy.

For IASI, European NWP centres may receive the full IASI spectra via EUMETCAST, so the choice of monitoring channels is made after the reception of the data. A total of 366 IASI channels are monitored at ECMWF this choice being based on the 300 channels used for distribution of IASI radiances via the GTS which is described in Collard (2007).

The 300 channels are chosen in a process with three main steps:

1. Removal of channels based on *ad hoc* criteria to avoid spectral regions with large uncertainties in the modelled spectra (i.e., pre-screening).
2. The main selection algorithm based on the information content of the measurements. This is comprised of a number of individual selection runs.

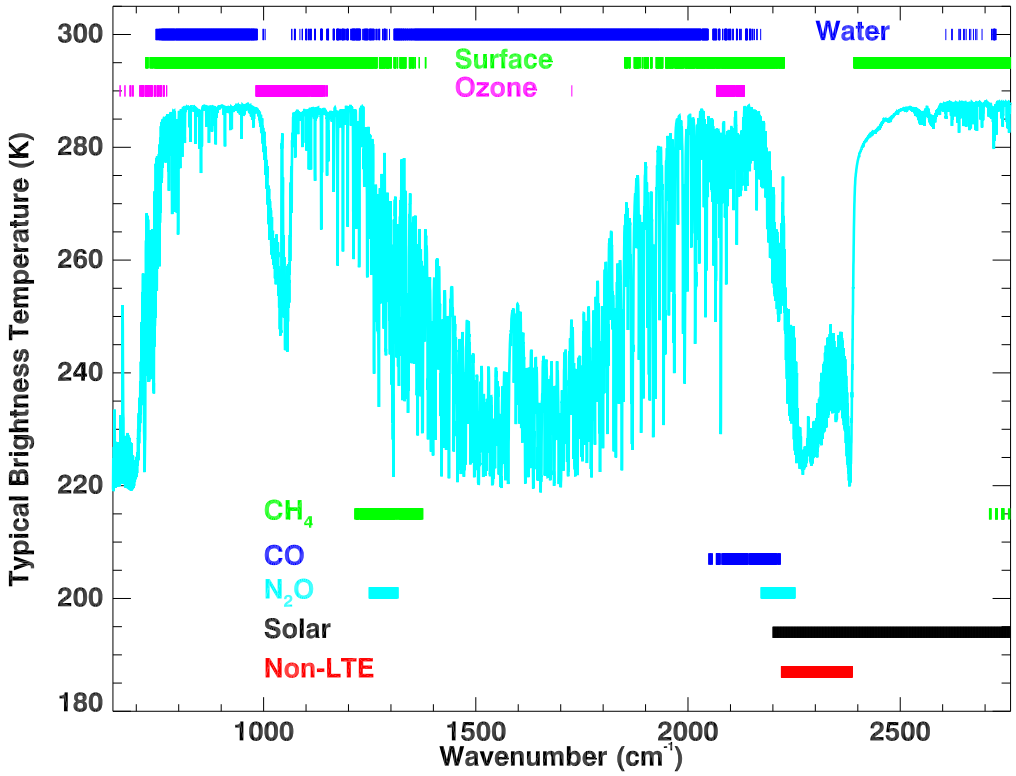

Figure 6: Blacklisted channels for channel selection. Channels with possible signals from CH_4, CO *or* N_2O *greater than 1K are blacklisted together with those channels in the 4.3*μ*m* CO_2 *band which are affected by non-LTE effects. Channels with large contributions from* H_2O, O_3, *the surface and solar irradiance are also indicated.*

3. *Ad hoc* addition of channels for specific purposes that could not be represented by the information content based selection algorithm.

The first step basically removes channels with significant signals from species that are not included in the state vector (CO, CH_4, and N_2O). Channels with signals due to H_2O, O_3, solar radiation or non-LTE effects may also be removed for some of the channel selection runs in the second step. These "blacklisted" channels are shown in Fig. 6.

The second step involves a number of runs of the automatic channel selection algorithm of Rodgers (1996, 2000). The various runs are to ensure that, for example, water vapour channels (which have sharp temperature Jacobians the form of which are very sensitive to the assumed H_2O profile) are not chosen to provide temperature information. The channel selection proceeds as follows:

1. Choose 30 channels in the 15μm CO_2 band considering their effect on temperature information only.
2. Choose a further 36 channels with Jacobians that peak in the troposphere in the 707–760cm^{-1} region of the 15μm CO_2 band, as experience with AIRS at ECMWF (e.g., Kelly and Thépaut, 2007) has shown that this region is the most beneficial to forecast scores.
3. Now considering, water vapour and temperature information together and including the 6.3μm water band in the available channels, choose a further 186 channels.

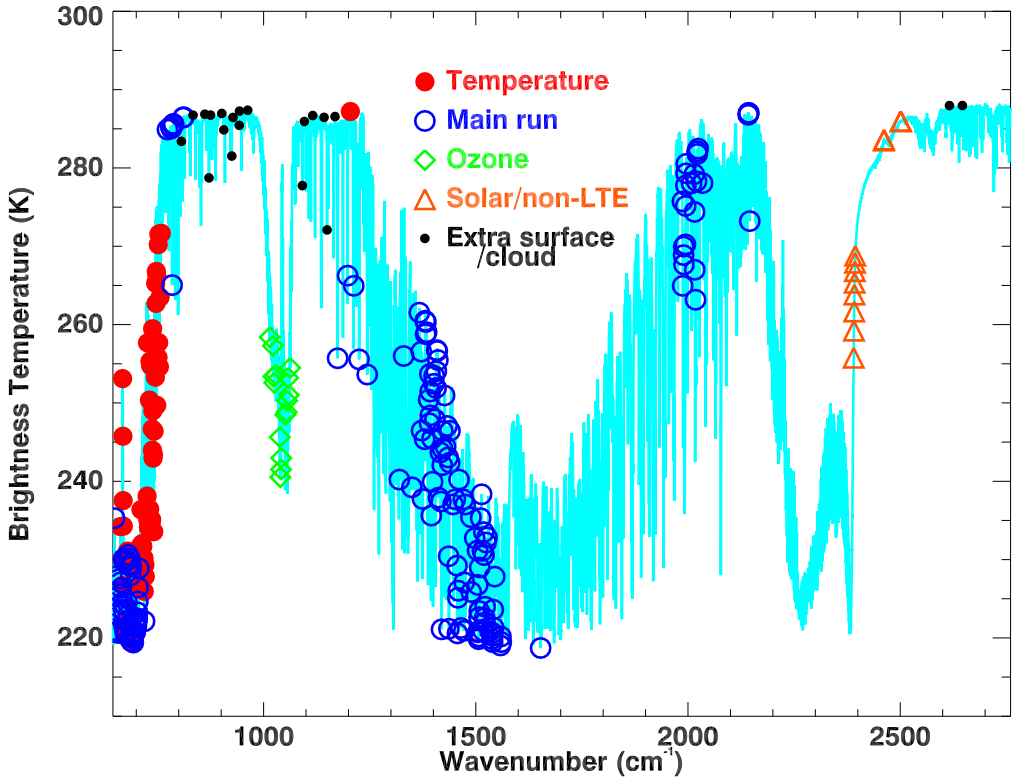

Figure 7: 300 channels chosen with the methodology described in the text.

4. Considering O_3 information only choose 15 more channels.
5. Considering solar-affected channels only add a further 13 channels.

The third step involves adding a further 20 channels in window regions and on weak absorption lines to be used for cloud detection and surface emissivity derivation. This makes the total number of channels chosen 300. These channels are shown in Fig. 7.

To these an additional 66 channels are added, these being: channels with similar properties to the HIRS channels (useful for monitoring purposes); channels requested by CNES for monitoring purposes; and 44 more channels in the 707–760cm^{-1} region, this time peaking in the lower stratosphere.

Figs. 8 and 9 show how the 324 AIRS and 300 IASI channels compare while Fig. 10 shows a comparison of the actively assimilated channels for AIRS and IASI in the ECMWF system for the 15μm band. The actively assimilated channels differ firstly through the purposeful addition of extra channels in the 13.1–14.1μm region and secondly because changes to the assimilation system in the stratosphere (Healy and Thépaut, 2006; Dee, 2007) now allow the stratospheric channels from AIRS and IASI to be included without degrading the system. This first implementation of the IASI assimilation does not include the active assimilation of water vapour channels.

2.2 Cloud Detection and Bias Correction

The ECMWF cloud detection algorithm works by taking the first guess departures (i.e., the difference between the observed brightness temperatures and brightness temperatures calculated from a good estimate of the at-

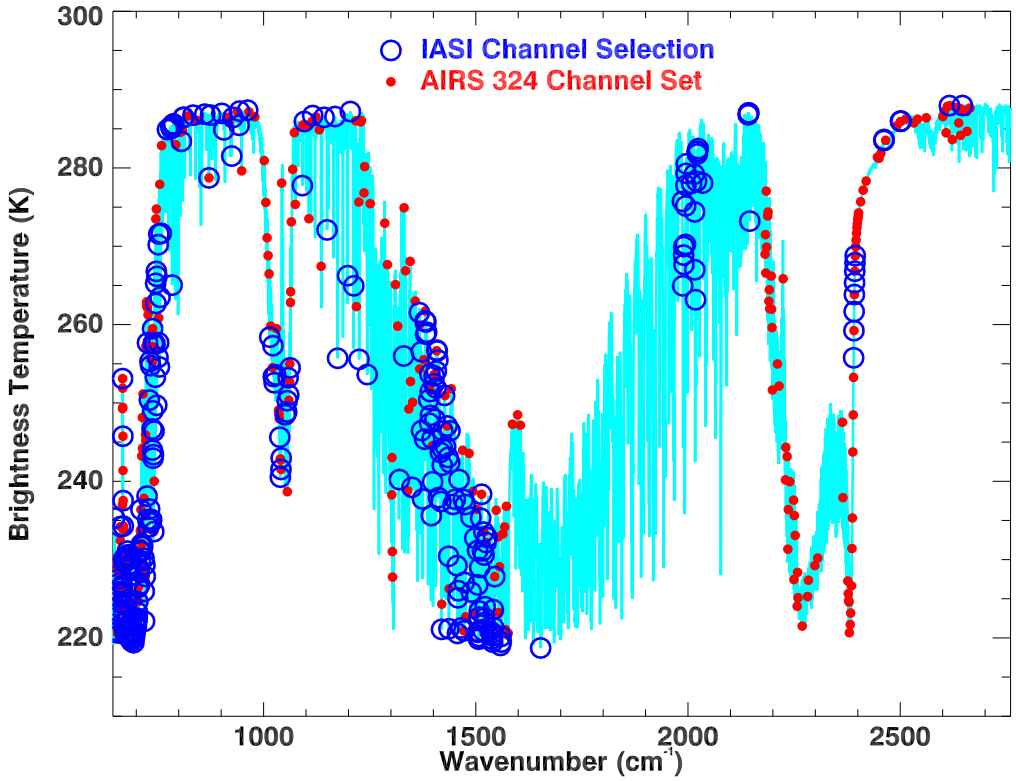

Figure 8: A comparison of the 324 channels distributed for AIRS and the 300 channels chosen for IASI.

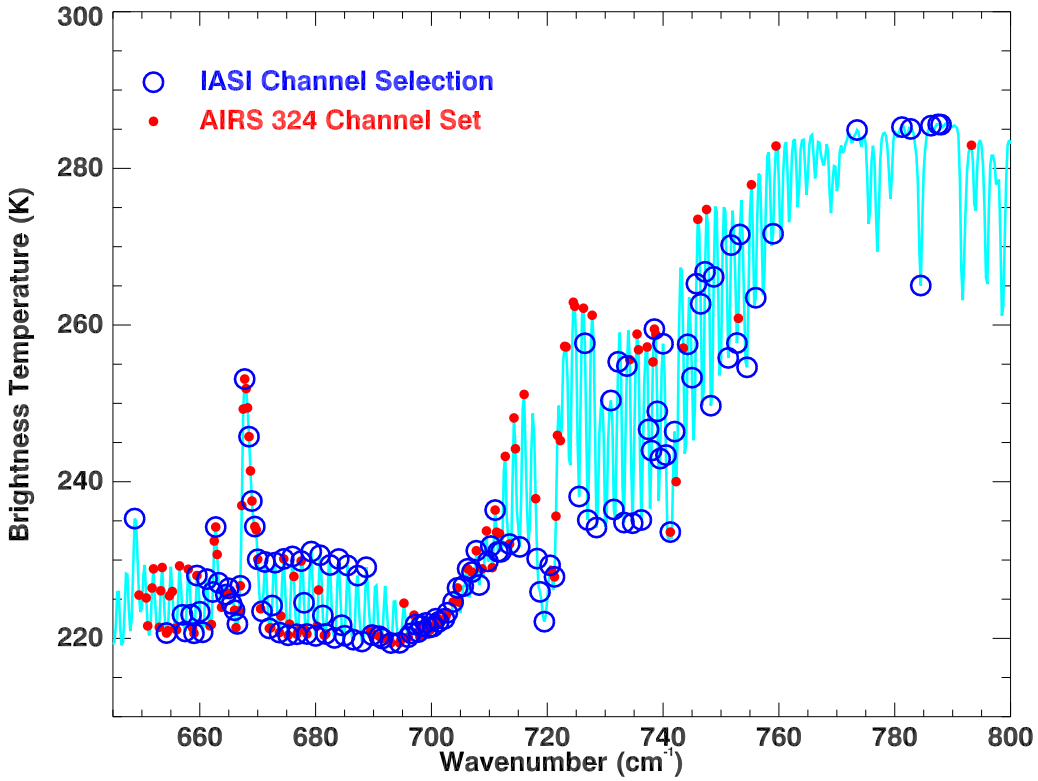

Figure 9: As Fig. 8, except focusing on the 15μm CO_2 band.

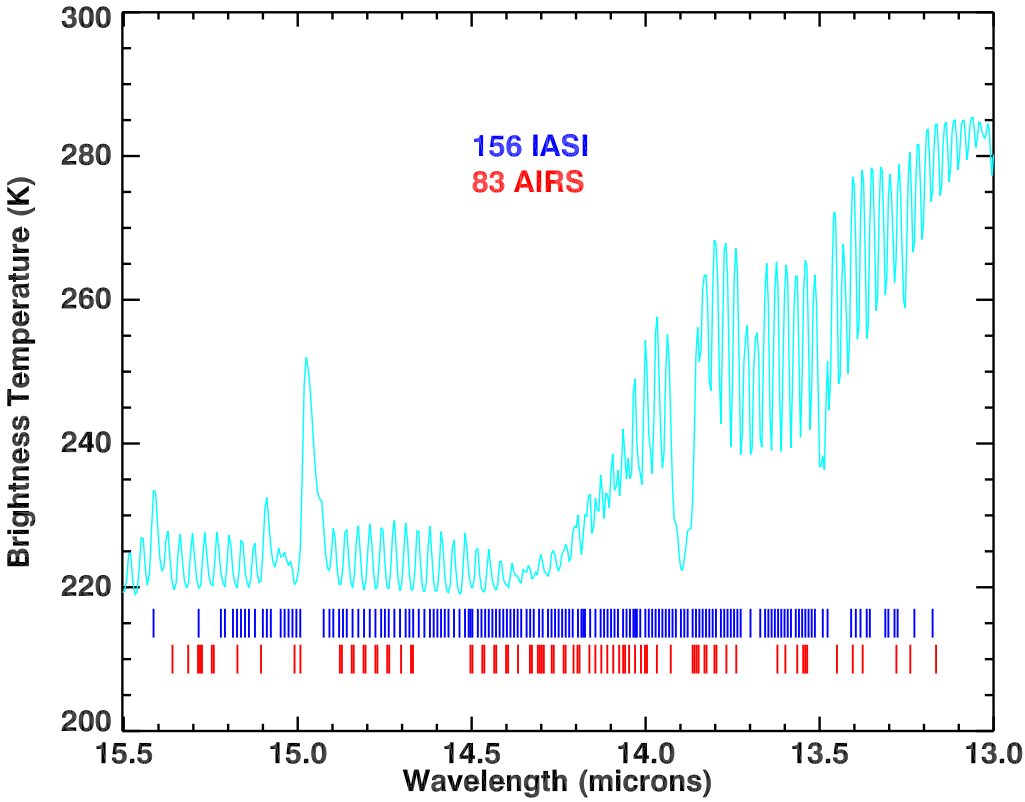

Figure 10: A comparison of actively assimilated channels for IASI and AIRS in the 15μm CO_2 band.

mospheric state - typically a 6-hour forecast from an NWP model) and looking for the signature of opacity that is not included in the clear-sky calculation (i.e. cloud or aerosol). To do this, the channels are first ordered according to their height in the atmosphere (with the highest channels first and the channels closest to the surface last) and then the resulting ranked brightness temperature departures are smoothed with a moving-average filter in order to reduce the effect of instrument noise. The algorithm then looks for a change in slope of the smoothed departures — a signal that would indicate the presence of a cloud. Most often, the change in slope will result in more negative departures as height rank increases (i.e., a cold cloud over a warm surface) but warm clouds over a cold surface can invert this and the possibility of such situations is considered. An illustration of the cloud detection algorithm for a single field of view is shown in Fig. 11. The typical number of channels identified as clear for a single 12-hour assimilation cycle is illustrated in Fig. 12.

The current configuration of cloud detection for AIRS at ECMWF divides the spectrum into five bands (long-wave CO_2 band; ozone; water vapour; 4.5μm CO_2 band and shortwave) with the first-guess departures in each band being used for its cloud detection. An alternative is used for IASI where the cloud height found for the 15μm CO_2 band is used to determine the unaffected channels in the other bands. This "cross-band" configuration attempts to remove uncertainties in the cloud detection in bands where the contribution to the first-guess departures from model error are more likely to be confused with the effects of cloud (this is particular problem with the H_2O band).

A detailed description of the cloud detection algorithm as used for AIRS in the ECMWF data assimilation system is given by McNally and Watts (2003). The algorithm is available via the NWPSAF website:

http://www.metoffice.gov.uk/research/interproj/nwpsaf/IR_aerosol_cloud_detect/index.html

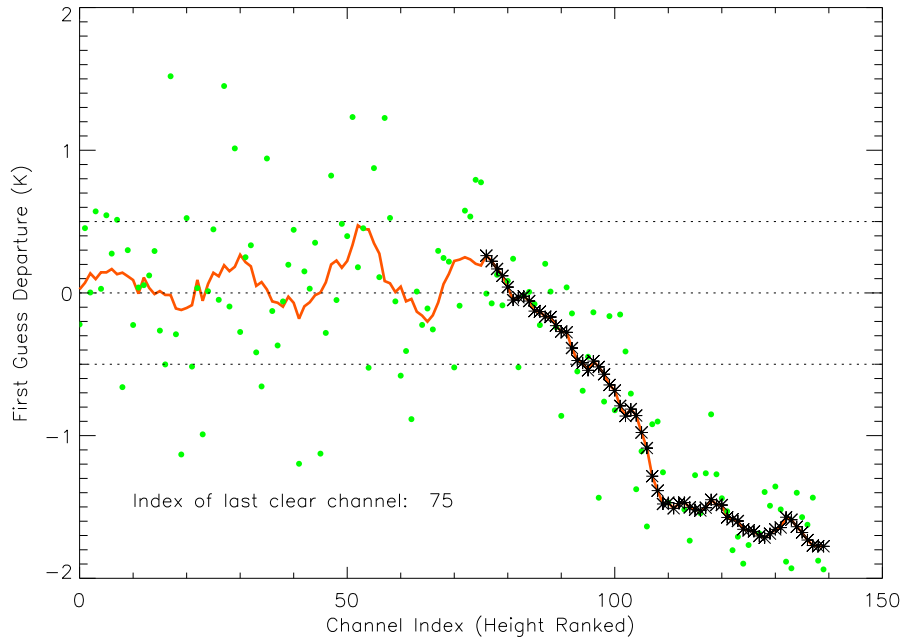

Figure 11: An illustration of the ECMWF cloud detection scheme in the 15μm CO_2 band. The first guess departures for each channel are green dots. A ten point moving average is applied (orange line) and the point were the mean gradient is greater than a predefined threshold is found. Below that point it is deemed to be cloudy (asterisks). A further requirement that the departures cannot be greater than 0.5K at the first clear point is enforced, as indicated by the doj 2tted lines. A higher height rank means the channel peaks lower in the atmosphere.

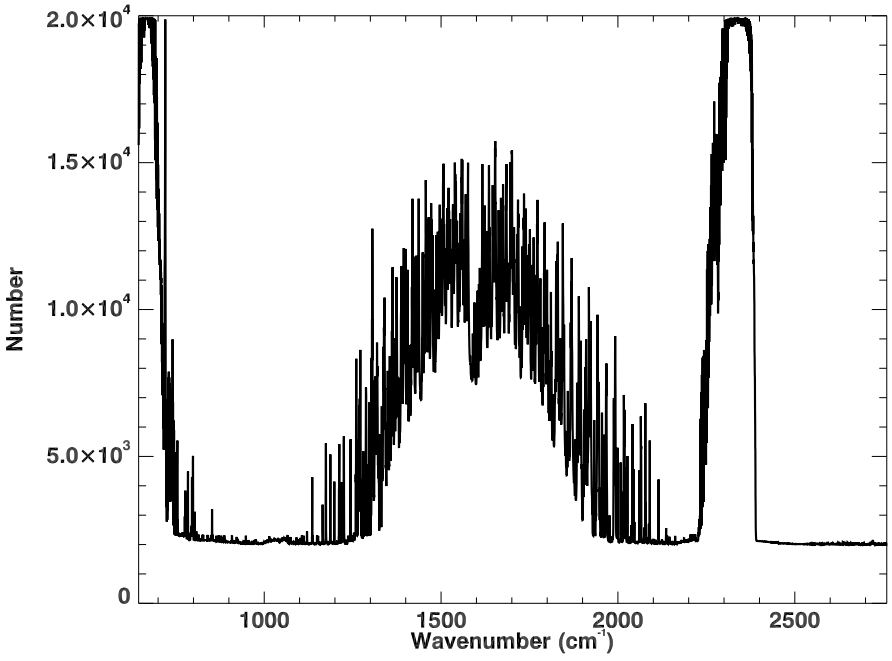

Figure 12: The number of IASI channels identified as clear by the ECMWF cloud detection scheme as a function of wavenumber for a 12-hour period. Channels which are not sensitive to the troposphere (around 670 and 2350 cm^{-1}) are designated as clear virtually all the time, while the incidence of clear channels drops to around 10% in window channels.

As the cloud detection relies on the bias-corrected first guess departures, it will depend on the bias correction applied. However in cloud-affected channels, the bias-correction coefficients will depend on the subset of observations that is deemed to be unaffected by cloud. There is therefore the potential for feedback between the cloud detection and bias-correction calculations.

A variational bias correction (VarBC) is used at ECMWF for most satellite data (Dee, 2005; Auligné *et al.*, 2007). In VarBC, bias correction coefficients are added to the state vector used in the variational assimilation. They are therefore estimated automatically during every assimilation cycle and this estimate benefits from the inclusion of information from all the other observation types in the system. For most AIRS and IASI channels, four airmass based parameters are used as predictors for the bias correction (the 1000–300hPa, 200–50hPa, 50–5hPa and 10–1hPa thicknesses) plus a cubic fit to the instrument view angle. For window channels, only the view angle bias correction is applied.

When a bias correction is updated frequently, there is a danger that the feedback between the cloud detection and the bias correction mentioned above will cause a long-term drift in the applied bias. This can possibly result in such unreasonably large corrections being applied that no clear channels are being selected at all. Auligné and McNally (2007) explored this interaction and identified strategies to ameliorate this effect (one being the removal of air-mass dependent predictors for the window channels of infrared sounders).

2.3 Forecast Impacts

The assimilation of both AIRS and IASI radiances result in positive impact on major meteorological fields. Fig. 13 shows the impact of assimilating AIRS observations on the 500hPa height scores, while Fig. 14 shows the same for IASI. These plots show the differences in 500hPa geopotential anomaly correlation forecast scores between the experiment and control runs normalised by the control run scores (positive values show that AIRS/IASI is improving the forecast). The error bars show 95% confidence intervals. In both cases significant positive impact is seen in one or both hemispheres.

Note that these two figures are for different time periods and so should not be compared directly. Furthermore, the IASI impact is on top of a system into which AIRS data is already assimilated.

Fig. 15 shows the spatial distribution of forecast improvements from IASI for the day-4 500hPa geopotential field.

Extensive Observation System Experiments (OSEs) by Kelly and Thépaut (2006) showed that AIRS was one of the two most important instruments in terms of impact on 500hPa height forecast accuracy. It had a marginally smaller impact than the three AMSU-A instruments (IASI was not available when these experiments were conducted), but out-performed a single AMSU-A.

3 Current Challenges

The current implementation of AIRS and IASI uses only a small fraction of the total available information in these measurements. Future advances in the use of these instruments will involve increasing the amount of information used through using more channels; more fields of view and greater weight on the assimilated observations. The following three sections briefly look at three specific areas where this should be addressed.

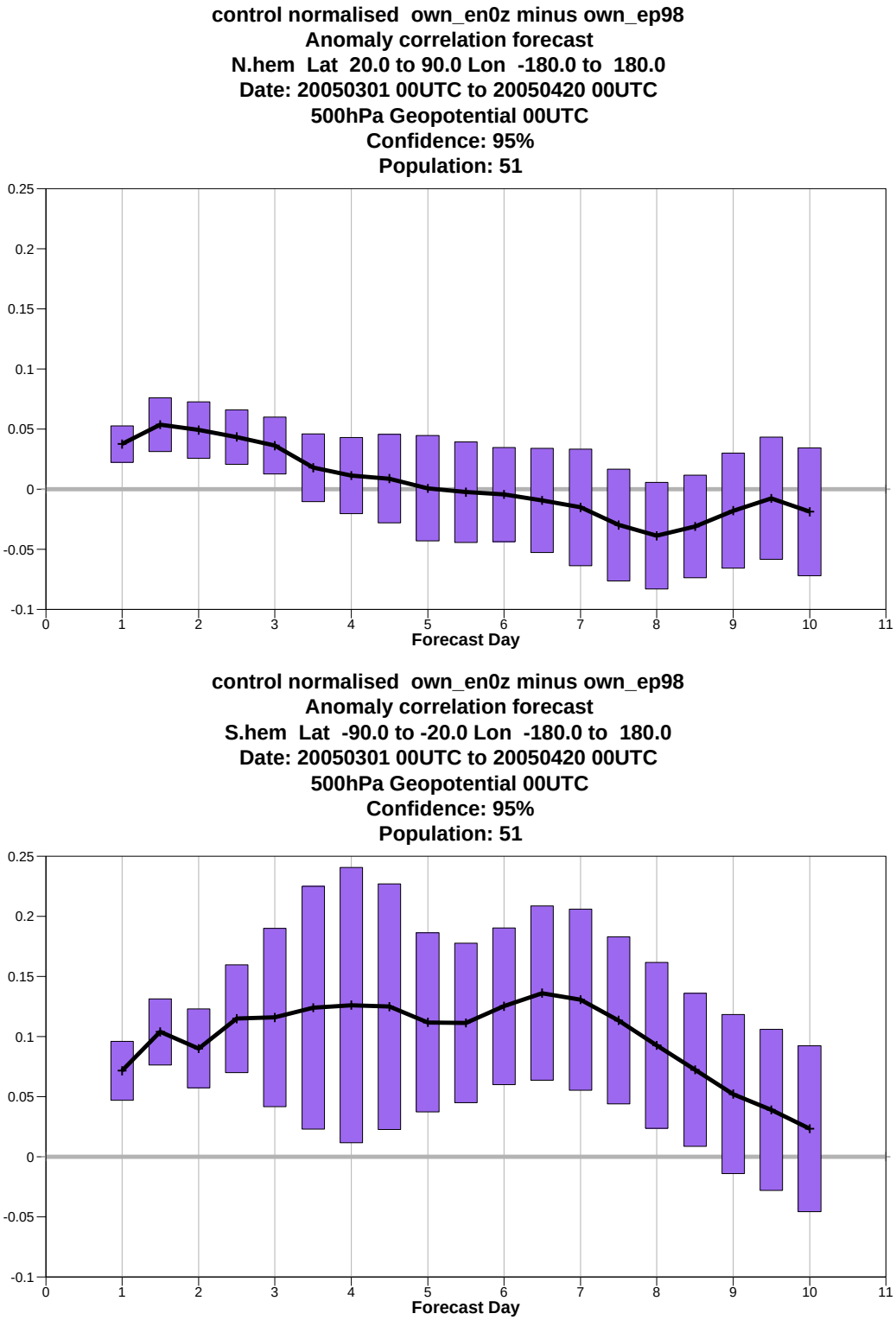

Figure 13: Impact of the assimilation of AIRS radiances on the 500hPa height forecasts. Positive values indicate improvement. The scores for each experiment are verified against its own analyses.

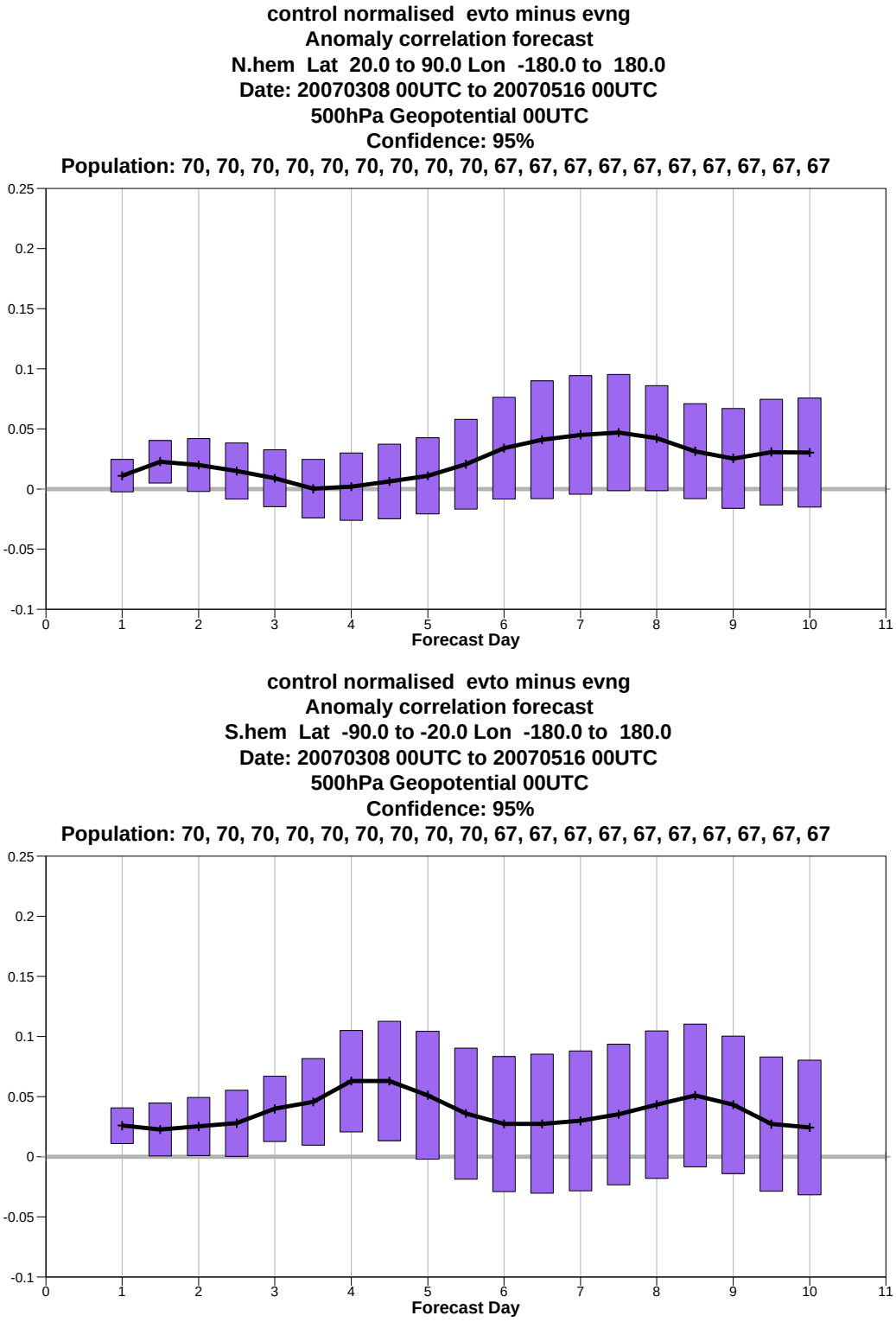

Figure 14: Impact of the assimilation of IASI radiances on the 500hPa height forecasts. Positive values indicate improvement. The scores are verified against the then operational system (which was not using the IASI observations but did include AIRS).

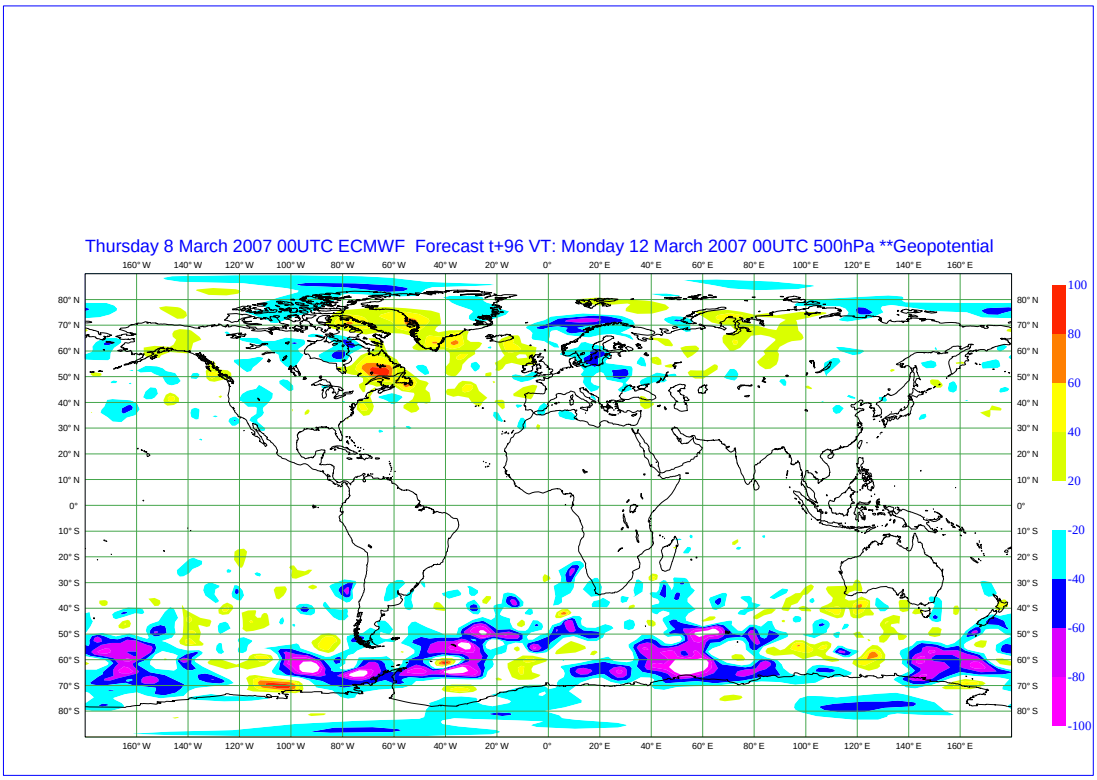

Figure 15: Root mean square difference in day-4 500hPa geopotential forecast error on the introduction of IASI radiances (8th March – 16th May 2007). Negative values indicate forecast improvement.

3.1 Assimilation of Water Vapour

The instrument noise for AIRS in the 6.3μm water vapour band is around 0.2K, yet the assumed observation error for this band is 2K. Experiments have shown that the fit to other observations (such as AMSU-B radiances) is degraded if the observation errors are reduced below this value. The situation at other NWP centres is similar: NCEP use 2.5K (J. Derber, priv. comm.) while the Met. Office use 4K (Cameron *et al.*, 2005).

Furthermore, as mentioned in Section 2.2, the cloud detection at ECMWF for AIRS channels in the 6.3μm water vapour band is reliant on the first-guess departures in the water vapour band itself. This has the result that observations in regions where the modelled water vapour error is high are often rejected as the cloud detection scheme can confuse the water vapour signal with that for cloud. The water vapour observations that are assimilated are therefore those which most agree with the model background.

A measure of the utility of an observation in an NWP system is whether it improves or degrades the (simultaneous) fit to other observations. Fig. 16 shows how varying the AIRS H_2O observation error to below 2K degrades the fit to the AMSU-B observations on NOAA-16. Similar results are seen for IASI.

Possible reasons for this need for error inflation include the fact that correlated observation and forward model error (including bias) is being approximated by an assumed diagonal error covariance and the possibility that model constraints are suppressing high resolution vertical structure or incorrectly distributing the increments in the horizontal or vertical.

One other possibility is that, as the water vapour channels have high sensitivity to temperature, the water

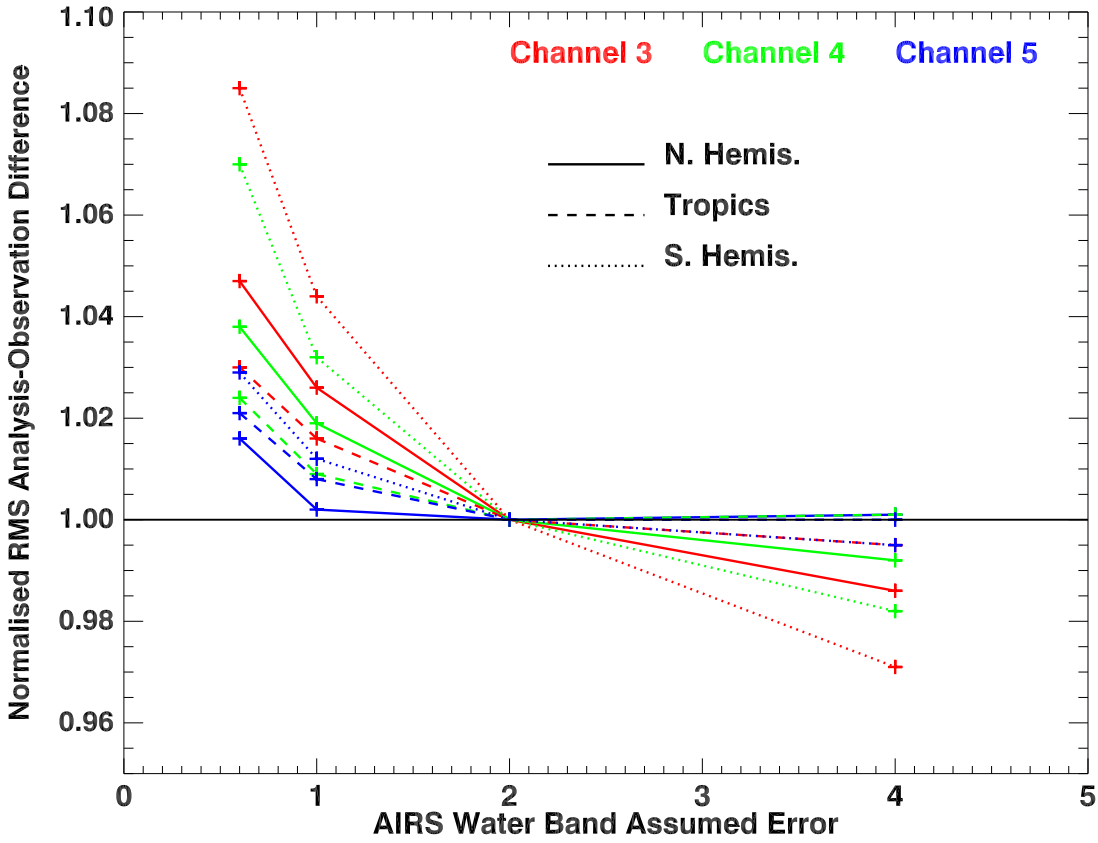

Figure 16: Root mean square analysis−observation differences for AMSU-B on NOAA-16 as a function of assumed observation error in the AIRS water vapour band. Each curve has been divided by the value when the observation error is the operational value of 2K. The fit to AMSU-B is seen to be degraded if the assumed AIRS H_2O *observation error is reduced below 2K*

vapour channels are affecting the temperature increments (which is undesirable as the form of the water vapour channels' temperature Jacobians is highly dependent on the assumed humidity profile). This has been found to be not a significant effect in our system.

The result of the above is that the weight given to water vapour channels is much lower than the simple consideration of the observational errors would imply. While such a configuration is found to give a small positive impact to the forecast scores, it is clear that there is potential to use the data more efficiently in this case. In particular, if the potential for high vertical resolution that these sounders promise is to be realised, one needs to have large numbers of channels with low real and assumed noise.

3.2 Cloud

Current operational NWP systems either assimilate infrared observations where the atmospheric column is completely clear or choose only channels that are unaffected by cloud. The percentage of available observations is reduced to 5–10% in the former case, while for the latter stratospheric channels are available 100% of the time with only 5–10% of window channels usable.

Strategies to increase the number of channels available in cloudy regions are generally either through attempting to remove the radiative effect of the cloud from the observations ("cloud clearing") or through the explicit

inclusion of cloud parameters in the state vector.

Cloud clearing (e.g., Li *et al.*, 2005) uses the spatial variability between adjacent fields of view to remove the cloud component from the observed radiances. Cloud-cleared radiances are thus a retrieved product rather then pure radiance observations. The errors associated with cloud cleared radiances are amplified relative to clear-sky radiances and are highly correlated between channels. These errors will also vary depending on the cloud situation being considered. Quality control and observation error specification are therefore important issues to consider when attempting to use these products in an NWP context. In addition, the influence of the *a priori* data used in the cloud-cleared radiance retrieval should be evaluated.

The inclusion of cloud properties in the state vector is at present an active area of research in the NWP community (e.g., Pavelin and English, 2006; Fourrié *et al.*, 2006; Bauer, 2007). These methods usually model the cloud as single grey layers with the expectation that greater sophistication can be introduced as research progresses. As with cloud-cleared radiances, increased; scene-dependent; spectrally-correlated errors result from this method — although these errors are more correctly identified as forward-model rather than observation errors. Quality control based on the cloud scenario that is inferred is also, once again, an important consideration.

3.3 Data Compression and Reconstructed Radiances

As there are at most only a few tens of pieces of independent information in each IASI spectrum, there is potential to represent these observations such that the bulk of the information is retained while reducing the data volume significantly.

The simplest method for reducing the data volume is channel selection as examined in Section 2.1. However, this method does not take account of the information contained in the majority of the sounders' channels.

For more efficient use of the information contained in kilochannel sounder radiances one must investigate methods for the representation of most of the information contained in the sounders' radiances in a smaller number of "channels" (by "channels", we are referring to the discrete quantities being assimilated rather than specifically channels as measured directly by the instrument). Such methods include super-channels, principal components reconstructed radiances and retrievals:

- Super channelling: Averaging similar IASI channels to produce a channel with similar properties except with much reduced random noise (Schlussel, 2005).
- Principal component analysis (PCA): Use a climatological set of IASI radiances to infer the principal modes of variability of the spectrum. These principal components (PCs) are associated with real atmospheric variations rather than random noise and the bulk of the atmospheric information in the spectrum is present in the first 100–200 PCs.
- Reconstructed radiances: Instead of directly assimilating principal components, use a truncated set of principal components to "reconstruct" the original spectrum. The result is that the full spectrum is used to estimate the true radiance in each channel but with noise greatly reduced. This may be considered a variant on super-channelling in that each reconstructed radiance is an estimate of the true channel radiance calculated by a linear combination of many channels.
- Retrievals: Represent the sounder spectrum as an atmospheric state (e.g., profiles of temperature, humidity etc.).

The assimilation of principal components and retrievals represents such a significant departure from the current practice of direct radiance assimilation that they are not considered a viable (or practical) option in the

near-term. Furthermore, the direct assimilation of radiances replaced retrieval assimilation to avoid existing problems with the specification of correlated retrieval errors and with the propagation of the retrievals' *a priori* information into the solution.

Super-channels and reconstructed radiances are both ways of compressing the information of the whole spectrum into a subset of "channels". The former is arguably a more physical approach and the latter more statistical.

Of these, reconstructed radiances are examined in most detail at ECMWF, primarily due to the availability of a near real time product for AIRS produced by NOAA/NESDIS.

Reconstructed radiances (Antonelli *et al.*, 2004) are formed through the evaluation of the amplitudes, $\mathbf{p}$, of the principal components, $\mathbf{L}$, of the observed spectrum. Here $\mathbf{L}$ is the set of N_p leading eigenvectors of the covariance matrix of a set of thousands of spectra. $\mathbf{p}$ is related to $\mathbf{y}$ (the noise normalised observed radiances with the mean observation subtracted) through.

$$\mathbf{p} = \mathbf{L^T y}$$

The reconstructed radiance $\tilde{\mathbf{y}}$ is then calculated from:

$$\tilde{\mathbf{y}} = \mathbf{L p} = \mathbf{L L^T y}$$

If we restrict $\tilde{\mathbf{y}}$ to a subset of N_R channels, by replacing the first $\mathbf{L}$ above with $\mathbf{L}_{\mathrm{NR}}$, those channels will contain all of the information present in the N_p principal components provided $\mathbf{L}_{\mathrm{NR}}$ has $\geq N_p$ positive singular values. The minimum criterion for this is that $N_R \geq N_p$ and in practice this criterion is usually sufficient.

The observation error for the reconstructed radiances can be derived from the raw observational error through

$$\varepsilon_{\tilde{\mathbf{y}}} = \mathbf{L}_{\mathrm{NR}} \mathbf{L}^T \varepsilon_{\mathbf{y}} + \varepsilon_{\mathbf{R}}$$

where $\varepsilon_{\mathbf{R}}$ is the error introduced on reconstructing the true (i.e., error free) spectrum (we may assume that sufficient principal components are used and that the training set for the principle components is sufficient that we may neglect this term). Therefore

$$Cov(\tilde{\mathbf{y}}) = E[\varepsilon_{\tilde{\mathbf{y}}} \varepsilon_{\tilde{\mathbf{y}}}^T] = \mathbf{L L}^T \mathbf{O L}^T \mathbf{L} + \mathbf{F}_R,$$

where $\mathbf{O}$ is the original observational error covariance matrix (in noise normalised radiance units) and $\mathbf{F}_R$ is the reconstruction error (which can be assumed to be negligible if sufficient principal components are used). Inspection of this transformation shows that the reconstruction process reduces the observational error but can also introduce significant inter-channel correlation. Note that if, as is the usual practice, the radiances are normalised by the true noise, $\mathbf{O}$=$\mathbf{I}$.

The reconstructed radiances dataset is supplied by NOAA/NESDIS in near real time for the same 324 channels as the real radiances. The radiances are calculated using the first 200 principal components of the climatological covariance of *observed* AIRS radiances (taken from the full set of observed data, i.e., clear and cloudy scenes). The principal components are derived from 1688 of the 2378 channels, as a number of noisy "popping" channels are omitted together with those channels around 4.3μm which are highly affected by non-LTE effects during the daytime. All data comes with a quality control flag which indicates whether the original spectrum has been reconstructed to within the noise limits.

Figs. 17 and 18 show a comparison between the first-guess departures for real and reconstructed radiances where the model fields are the same. The standard deviations of the reconstructed radiances' first-guess departures are significantly reduced for all those channels where instrument noise is expected to be a significant

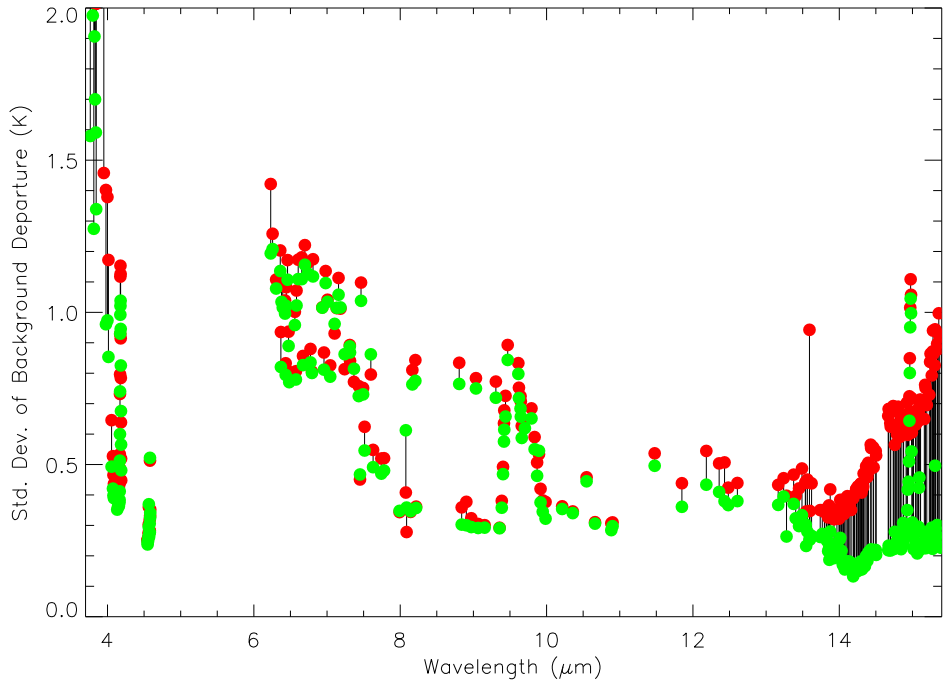

Figure 17: A comparison of the standard-deviations of clear-sky departures from the same model first-guess for real (red) and reconstructed (green) radiances. Significant "denoising" is seen in the 15μm band where instrument noise is dominant over model error. The apparent increase in departure standard deviation for the channel at 8.07μm is an artifact arising from the cloud detection scheme.

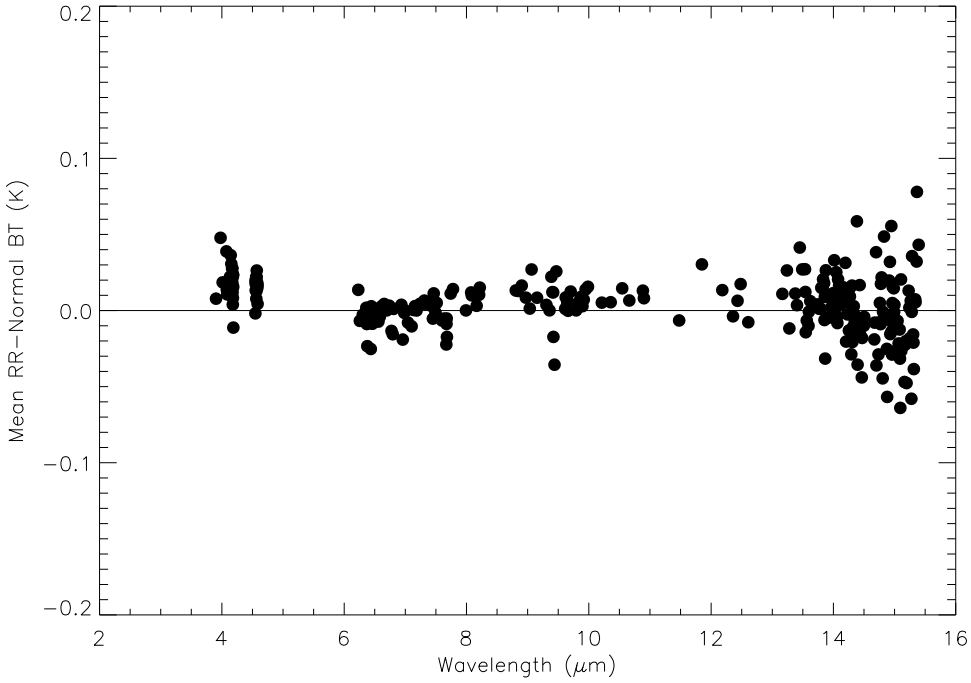

Figure 18: The difference between the mean clear-sky departures from the same model first-guess for real and reconstructed radiances.

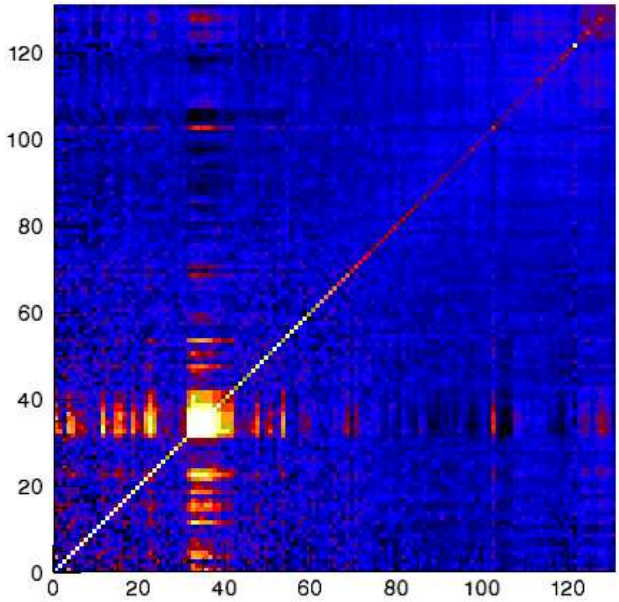

Figure 19: The covariance matrix of the first-guess departures for the first 120 channels of the 324 channel subset (covering the region 649–739cm^{-1}) for real radiances. The instrument noise is seen to be very close to diagonal while off-diagonal covariances are only significant for channels that sound the stratosphere - where the model error outweighs the instrument noise.

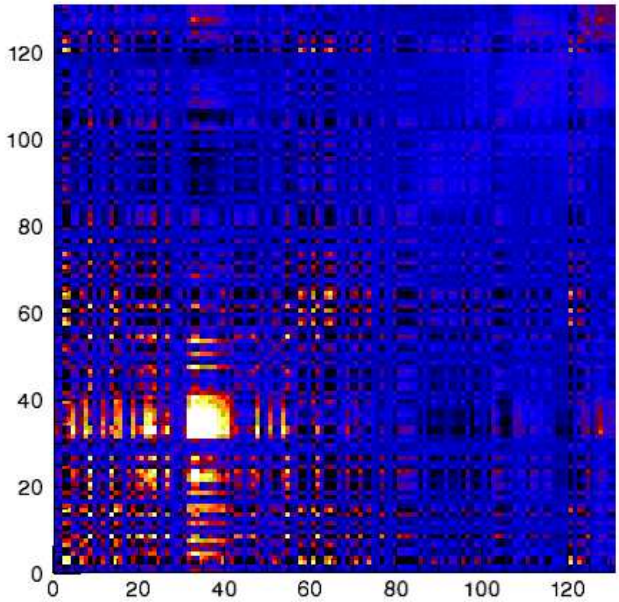

Figure 20: As Fig. 19 except for reconstructed radiances, the colour scale is the same. The diagonal noise is seen to be greatly reduced where instrument noise is dominant but this noise is now correlated between similar channels.

contributor to the total departure. The biases are unchanged, as the effect of reconstruction is to smooth random noise rather than change the mean radiances.

As mentioned above, one expects the errors in the reconstructed radiances to be correlated between channels. To verify this we can compare the covariance matrix of the first-guess departures of used data for real radiances with that for reconstructed radiances. The result for the first 120 AIRS channels in the 324 channel subset is shown in Figs. 19 and 20. For real radiances the departures are generally uncorrelated except where vertically correlated model errors in the stratosphere (e.g., around channel 35) are significant. It can be seen that the reconstruction process introduces significant additional correlations into the departures.

Extensive experimentation has been carried out on the assimilation of reconstructed radiances with a variety of assumed observation errors. So far, none has been found to give a significant positive impact above the (already positive) impact of the real AIRS radiances, but experiments continue.

4 Conclusions

AIRS and IASI are important instruments in the ECMWF data assimilation system. In particular these instruments provide useful information from their temperature sounding channels sensitive to the upper-troposphere and lower-stratosphere.

Kilochannel infrared sounders such as AIRS and IASI have the potential to provide information to the NWP systems with high accuracy and vertical resolution. For this to be achieved, the information present in the large number of channels with overlapping Jacobians and low noise needs to be presented to the model in an efficient manner. Efficient quality control, particularly when considering the treatment of clouds, is also a requirement.

Future advances in the assimilation of these instruments will focus on increasing the use of these data in spatial (through, for example, better use of cloudy fields of view) and spectral domains plus more optimal weighting.

Acknowledgements

The author acknowledges the important contributions of Tony McNally, Sean Healy, Marco Matricardi, Rossana Dragani and Richard Engelen.

References

ANTONELLI, P., H.E. REVERCOMB, L.A. SROMOVSKY, W.L. SMITH, R.O. KNUTESON, D.C. TOBIN, R.K. GARCIA, H.B. HOWELL, H.-L. HUANG, AND F.A. BEST (2004). A principal component noise filter for high spectral resolution infrared measurements, *J. Geophys. Res.*, **109**, D23102–23124.

AULIGNÉ, T., A. P. MCNALLY AND D. P. DEE (2007). Adaptive bias correction for satellite data in a numerical weather prediction system. *Q.J.R. Meteorol. Soc.*, **133**, 631–642.

AULIGNÉ, T. AND A. P. MCNALLY (2007). Interaction between bias correction and quality control. *Q.J.R. Meteorol. Soc.*, **133**, 643–653.

AUMANN, H.H., M.T. CHAHINE, C. GAUTIER, M.D. GOLDBERG, E. KALNAY, L.M. MCMILLIN, H. REVERCOMB, P.W. ROSENKRANZ, W.L. SMITH, D.H. STAELIN, L.L. STROW, J. SUSSKIND (2003). AIRS/AMSU/

HSB on the Aqua mission: design, science objectives, data products, and processing systems. *IEEE T Geosci Remote,* **41**, 253–264.

BAUER, P. (2007). The assimilation of cloud and rain-affected observations at ECMWF. In *Proceedings of the ECMWF Seminar on 'Recent developments in the use of satellite instruments in numerical weather prediction' 3–7 Sept. 2007.*ECMWF Report, Reading, U.K.

BLOOM, H.J. (2001) The cross-track infrared sounder (CrIS): a sensor for operational meteorological remote sensing. *Proc. Geoscience and Remote Sensing Symposium, 2001.* **3**, 1341 - 1343.

CAMERON, J., A. COLLARD AND S. ENGLISH (2005). Operational use of AIRS observations at the Met. Office. *Proceedings of the Fourteenth International TOVS Study Conference, Beijing, China. 25th–31st May 2005.*

CHALON, G., F. CAYLA AND D. DIEBEL (2001). IASI: An Advanced Sounder for Operational Meteorology. *Proceedings of the 52nd Congress of IAF, Toulouse France, 1-5 Oct. 2001*

COLLARD, A.D. (2001). Assimilation of IASI and AIRS data: Information Content and Quality Control. In *Proceedings of the ECMWF Seminar on 'Exploitation of the new generation of satellite instruments for numerical weather prediction' 4–8 Sept. 2000.*ECMWF Report, Reading, U.K.

COLLARD, A.D., AND S.B. HEALY (2003). The combined impact of future space-based atmospheric sounding instruments on numerical weather-prediction analysis fields: A simulation study. *Q.J.R. Meteorol. Soc.*, **129**, 2741–2760.

COLLARD, A.D. (2007). Selection of IASI Channels for use in Numerical Weather Prediction. *ECMWF Technical Memorandum No. 532.* (*To appear in Q.J.R. Meteorol. Soc.*)

DEE, D.P. (2005). Bias and data assimilation. *Q.J.R. Meteorol. Soc.*, **131**, 3323-3343.

DEE, D. (2007). Importance of satellites for stratospheric data assimilation. In *Proceedings of the ECMWF Seminar on 'Recent developments in the use of satellite instruments in numerical weather prediction' 3–7 Sept. 2007.*ECMWF Report, Reading, U.K.

FOURRIÉ, N., M. DAHOUI, AND F. RABIER (2006). Towards the assimilation of AIRS cloudy radiances. *Proceedings of the Fifteenth International TOVS Study Conference, Maratea, Italy. 4th–10h October 2006.*

GOLDBERG, M.D., Y. QU, L.M. MCMILLIN, W. WOLF, L. ZHOU AND M. DIVAKARLA (2003). AIRS near-real-time products and algorithms in support of operational numerical weather prediction. *IEEE T Geosci Remote,* **41**, 379–389.

HANEL, R.A., B. SCHLACHMAN, D. ROGERS AND D. VANOUS (1971). Nimbus 4 Michelson interferometer. *Appl. Opt.,* **10**, 1376–1382.

HANEL, R., B. CONRATH, D. GAUTIER, P. GIERASCH, S. KUMAR, V. KUNDE, P. LOWMAN, W. MAGUIRE, J. PEARL, J. PIRRAGLIA, C. PONNAMPERUMA AND R. SAMUELSON (1977). The Voyager infrared spectroscopy and radiometry investigation. *Space Sci. Rev.,* **21**, 129–157.

HARRIES, J.E., H.E. BRINDLEY, P.J. SAGOO AND R.J. BANTGES (2001). Increases in greenhouse forcing inferred from the outgoing longwave radiation spectra of the Earth in 1970 and 1997. *Nature*, **410**, 355–357.

HEALY, S.B. AND J.-N. THÉPAUT (2006). Assimilation experiments with CHAMP GPS radio occultation measurements. *Q.J.R. Meteorol. Soc.,* **132**, 605–623.

JOINER, J., E. BRIN, R. TREADON, J. DERBER, P. VAN DELST, A. DA SILVA, J. LE MARSHALL, P. POLI, R. ATLAS, D. BUNGATO AND C. CRUZ (2007). Effects of data selection and error specification on the assimilation of AIRS data. *Q.J.R. Meteorol. Soc.,* **133**, 181–196.

KELLY, G. AND J.-N. THÉPAUT (2006). THE RELATIVE CONTRIBUTIONS OF THE VARIOUS SPACE OBSERVING SYSTEMS TO THE ECMWF FORECAST SYSTEM. *Proceedings of the Fifteenth International TOVS Study Conference, Maratea, Italy. 4th–10th October 2006*.

KELLY, G. AND J.-N. THÉPAUT (2007). EVALUATION OF THE IMPACT OF THE SPACE COMPONENT OF THE GLOBAL OBSERVING SYSTEM THROUGH OBSERVING SYSTEM EXPERIMENTS, ECMWF NEWSLETTER. NO. 112 AUTUMN 2007

KOBAYASHI, H., A. SHIMOTA, C. YOSHIGAHARA, I. YOSHIDA, Y. UEHARA AND K. KONDO (1999). Satellite-borne high-resolution FTIR for lower atmosphere sounding and its evaluation. *IEEE T Geosci Remote,* **37**, 1496–1507.

LI J., C.-Y. LIU, H.-L. HUANG, T.J. SCHMIT, X. WU, W.P. MENZEL AND J.J. GURKA (2005). Optimal cloud-clearing for AIRS radiances using MODIS. *IEEE T Geosci Remote,* **43**, 1266–1278.

MCNALLY, A.P. (2002). A note on the occurrence of cloud in meteorologically sensitive areas and the implications for advanced infrared sounders. *Q.J.R. Meteorol. Soc.],* **128**, 2551–2556.

MCNALLY, A.P. AND P.D. WATTS (2003). A cloud detection algorithm for high-spectral-resolution infrared sounders. *Q.J.R. Meteorol. Soc.,* **129**, 2411–2323.

MCNALLY, A.P., P.D. WATTS, J.A. SMITH, R. ENGELEN, G.A. KELLY, J.-N. THÉPAUT AND M. MATRICARDI (2006). The assimilation of AIRS radiance data at ECMWF. *Q.J.R. Meteorol. Soc.],* **132**, 935–957.

PAVELIN, E.G. AND S.J. ENGLISH (2006). Plans for the assimilation of cloud-affected infrared soundings at the Met Office. *Proceedings of the Fifteenth International TOVS Study Conference, Maratea, Italy. 4th–10th October 2006. Submitted to Q.J.R. Meteorol. Soc.*

PRUNET, P., J.-N. THÉPAUT AND V. CASSÉ (1998). The information content of clear sky IASI radiances and their potential for numerical weather prediction. *Q.J.R. Meteorol. Soc.,* **124**, 211–241.

RABIER, F., E. KLINKER, P. COURTIER AND A. HOLLINGSWORTH (1996). Sensitivity of forecast errors to initial conditions. *Q.J.R. Meteorol. Soc.,* **122**, 121–150.

RODGERS, C.D. (1996). Information content and optimisation of high spectral resolution measurements. *SPIE, 2380, Optical spectroscopic techniques and instrumentation for atmospheric and space research II, Paul B. Hays and Jinxue Wang eds.,* pp. 136–147.

RODGERS, C.D. (2000). Inverse methods for atmospheres: Theory and Practice. *World Scientifi c Publishers, Singapore.*

SAUNDERS, R.W. (2001). Assimilation of IASI and AIRS data: Forward Modelling. In *Proceedings of the ECMWF Seminar on 'Exploitation of the new generation of satellite instruments for numerical weather prediction' 4–8 Sept. 2000.*ECMWF Report, Reading, U.K.

W.L. SMITH, H.E. REVERCOMB, R.O. KNUTESON, F.A. BEST, R. DEDECKER, H.B. HOWELL, AND H.M. WOOLF (1995). Cirrus cloud properties derived from high spectral resolution infrared spectrometry during FIRE Ⅱ. Part I: The High Resolution Interferometer Sounder (HIS) systems. *J. Atmos. Sci.,* **52**, 4238–4245.

SCHLUSSEL, P. (2005). Super-channel selection for IASI retrievals. *Proceedings of the Fourteenth International TOVS Study Conference, Beijing, China. 25th–31st May 2005.*

SUSSKIND, J., C.D. BARNET, AND J.M. BLAISDELL (2003). Retrieval of atmospheric and surface parameters from AIRS/AMSU/HSB data in the presence of clouds. *IEEE Trans. Geosci. Remote Sensing,* **41**, 390–409.